14

Simulation of On-Board Supercapacitor Energy Storage System for Tatra T3A Type Tramcars

Leonards Latkovskis, Viesturs Brazis and Linards Grigans
Institute of Physical Energetics
Riga Technical University
Latvia

1. Introduction

The most efficient and low emission kind of public transport is a rail transport. Tram based light rail transit has been chosen by city government as the main urban transportation solution in Riga. However, the running trams in Riga have been produced in 1976-1987 (type T3 with a rheostat accelerator) and 1988-1990 (type T3M with a thyristor drive).
In Eastern Europe and even in old EU countries for many decades old trams with DC traction drive have still been in use for the reasons that the exploitation resource of mechanical parts of rolling stocks in the rail electric transport is mostly 30-50 years and that the cost of a new tramcar is approximately 1-2.5 million Euros, which makes it difficult for many transport operator companies to renew the old fleet before its complete physical wear. Therefore, the reconstruction of tramcars has been made to prolong their exploitation period by 10-20 years, with replacing the traction equipment by newer and more energy-efficient one, providing regenerative braking that allows 20-40% of the consumed energy to be returned (Rankis, I. & Brazis, V., 2000). Although the best energy saving and improvement of tramcar performance could be achieved by replacing a DC drive with an asynchronous one, the rise in the cost of the electrical part seldom pays off in the 10, maximum 20 post-reconstruction years. This forces to restrict the renovation to replacement of rheostat and thyristor control systems by transistor ones, with old DC traction motors left (Joller, J., 1998).
A large reconstruction of 191 T3 type tramcars to T3A took place in the Riga city from the 1998 to 2002. The renewed tramcars obtained regenerative braking capability and can provide reduction of the energy consumption up to 40%.
However, the regenerative braking energy is not completely used in typical existing traction drive system because none of the substations is equipped with a reversible rectifier. The real energy saving strongly depends on other trams connected to the same section of overhead line. If a number of trams are connected to the DC overhead, part of the regenerative braking energy could be distributed to other trams when they are operated in traction mode, but in the case of several tram simultaneous breaking the energy could not be utilized and is wasted in braking rheostat. It is often impossible for the tramcars to instantly consume regenerative energy at low traffic density in off-peak hours and on easily loaded lines, since in the overhead supplying zone of a single traction substation at one tram's braking other

trams infrequently can simultaneously utilise the energy in the traction mode (Barrero, R. et al, 2008 A) or even are not located in this net supplying zone.
Using methodology described in (Latkovskis, L. & Grigans, L., 2008 A) the wasted energy for two substations feeding approximately 3 km long distances of overhead line of tram lines № 6 and № 11 has been estimated (Latkovskis, L. & Grigans, L., 2008 B). It yields 147MWh and 125MWh per year correspondingly. Taking into account that there are 34 substations in Riga, the total wasted energy is estimated by order of 3GWh per year.
There are three basic solutions for saving the untapped braking energy:

- modification of substations by replacing old rectifiers with reversible ones;
- installation of stationary energy storages at substations or near the optimal connection points of the overhead power supply line;
- installation of onboard energy storage devices on the electric vehicles.

Equipment of substations with reversible rectifiers has several drawbacks:

- the necessity to modify substations, including replacement of power transformers or installation of additional ones;
- simple reversible thyristor rectifiers have a low power factor and distorted line current, while transistor rectifiers with a sinusoidal current waveform are rather complicated and expensive;
- none of substation reversible rectifier types are able to shave peak energy consumption, on the contrary, they increase the power system voltage fluctuations with opposite regenerated energy flow;

To obtain the useful utilization of regenerative energy and reduce overall energy consumption, braking energy should be temporarily saved in energy storage system (ESS) until the correspondent power consumer is connected to the overhead line. Only energy storage system could join the regenerative energy storage task with peak power reduction and overhead voltage stabilization. The ESS could be installed stationary in substation, weak spots of network or onboard on vehicle.
In difference from heavy rail transport with predictable acceleration and deceleration areas mostly near stations, curves, hills, switches etc., the city traffic conditions with low speeds, frequent acceleration and sudden braking is characterised by dissipated starting and braking zones along transport network. The energy transfer from a tramcar to the other vehicle or substation at a distance from several hundred meters up to few kilometres is coupled with considerable energy losses, which decreases the power saving up to 10% (Rankis, I. & Brazis, V., 2000). Therefore the most effective way of the regenerative energy using without transfer losses is installation the onboard ESS.
The modern trams have increased dynamical properties and average speed, which leads the highest current constraints on overhead line and introduce large voltage drops in the traction mode (Destraz, B. et al, 2007). The starting power peaks represent a problem of availability of enough power feeding network, otherwise large voltage drops occur, which significantly reduce tram dynamic performance parameters. Overhead resistance increases with distance from substation, which causes permanent undervoltage far from substation and eliminates the stationary ESS effect to voltage stabilising. Only onboard ESS provides direct stored energy applying to the place of consuming, which improve dynamic behaviour of the vehicle by else having the same acceleration in weaker network or higher acceleration in well feed overhead lines. Onboard ESS allows increasing the number of trams without

need of building new expensive substations, which is important in the case if traffic increasing is necessary periodically for limited time.

Important advantage of onboard ESS is autonomous traction feature and full regenerative braking energy storage possibility, restricted by storage capacity only. The braking energy transfer to onboard ESS is independent from overhead availability, which is especially important in Riga due to specific Tatra T3A type tramcar power circuit drawbacks and overhead network construction. The Riga overhead network has a lot of tram and trolleybus crossings and disconnections with neutral parts, where energy transfer is impossible. Also the regenerative braking is not allowed on automated rail and overhead wire frogs, because the travel direction is switched by high or low tram load. Future planned tram tunnels and introduction of shared tram and trolleybus operation on public transport lines increases the demands for tram autonomous traction possibility with limited speed and distance to ensure fast vehicle removing from intersections, tunnels and other places, where it disturbs other traffic.

One of the most perspective energy storage devices is a large capacity supercapacitor battery which is chosen for tram ESS. In comparison with chemical accumulator batteries and rotating fly-wheels the supercapacitors have better charge and discharge dynamic characteristics despite the smaller total energy capacity. The supercapacitor advantages are also independence of parameters on the environment temperature, smaller weight, lower cost and dimensions than other types of energy storage system type.

Therefore the most attention is paid to the maximum storage of regenerative energy, applying as simple as possible technical solutions, which would allow the least rise in the cost of traction equipment without decreasing the tramcar operation safety. Such storage is achieved using a single-stage pulse converter without intermediate DC conversions (Latkovskis, L. & Bražis, V. 2007). Due to lack of speed sensor and difficult access to traction and braking signal outputs of the tram T3A, the control system of ESS is developed independent of the tram controller. In difference from ESS with speed sensor (Barrero, R.; et al., 2008 A), which must be recommended for brand new vehicles, the proposed solution with independent ESS converter control system could be easily connected to existing tram without reengineering traction circuit and tram control system hardware and software. In such system are two independent PWM unlinked clock signal for tram DC converter and ESS current controller. As the ESS is connected to the filter capacitor of tram DC converter therefore interference of DC converter and ESS current controller has been investigated in both synchronous and asynchronous operation modes of the both converters.

The ESS straightforward constant current charging has compatibility problems with line parameters (Sejin N.; et al., 2008). Supercapacitor charging with a constant power requires incorporation of the ESS control system into vehicle traction drive and modifying the last (Szenasy, I., 2008). The charging algorithm with constant filter capacitor voltage is chosen for providing the automatic whole braking energy saving without significant modification of the existing tram power circuit.

The PSIM and Matlab/Simulink simulation is performed for tramcar starting and braking processes in different situations with and without another tram connected to the overhead line and for autonomous traction mode.

The DC PWM tram converter is represented in two versions – as a continuous and a pulsed current source. By applying the pulsed current PSIM model the interference between ESS and DC PWM tram converter is investigated.

2. Power circuit of ESS and T3A tramcar traction drive

While connecting supercapacitor energy storage system to the existing T3A tramcar power scheme it is necessary to take into account that it must provide:

- two-way voltage boost/buck energy interchange between the T3A power circuit and the supercapacitor,
- smoothed charge/discharge current of the supercapacitor,
- smoothed and radio-frequency filtered line current,
- controllable initial charge of the supercapacitor,
- protection of the supercapacitor against overcurrents caused by overhead short circuits.

A simple solution of ESS power stage may be achieved connecting it to the tram filter capacitor (Latkovskis, L. & Bražis, V., 2007) at supercapacitor's voltage always being lower than the filter capacitor's voltage V_{Cf} (Rufer, A., 2003), (Barrero, R.; et al., 2008 B). A simplified circuit diagram of the energy storage system and its connection to the T3A tramcar power circuit is shown in Fig.1.

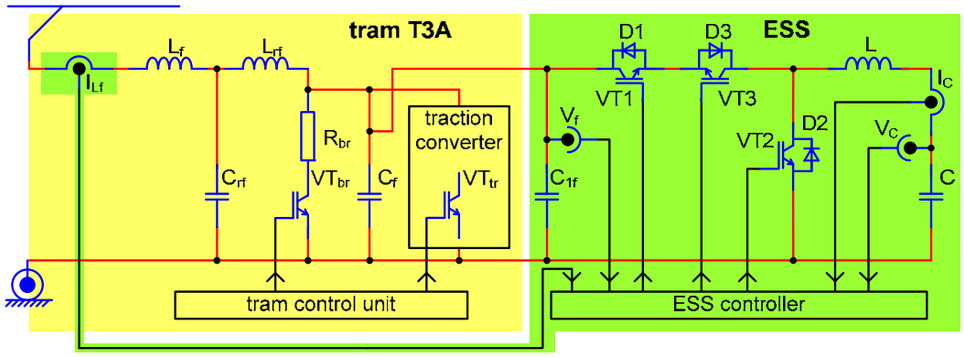

Fig. 1. A simplified circuit diagram of ESS and its connection to the T3A tramcar power circuit

The ESS consists of supercapacitor *C* and bidirectional DC/DC power converter. IGBT *VT1* and diode *D2* works as a voltage buck converter in the supercapacitor *C* charging mode, but *VT2* and *D1*, at switched on *VT3*, as a voltage boost converter in the supercapacitor *C* discharging mode. IGBT *VT3* is necessary for protection of the supercapacitor *C* in the cases, when a short circuit or undervoltage occurs in the overhead line or tram traction converter. To prevent overcurrents and uncontrolled discharge of supercapacitor, *VT3* is switched off when ESS input voltage is lower than supercapacitor voltage.

The ESS is connected to the tram's filter capacitor C_f =5100μF which is therefore also used as a basic element for the buck/boost converter of ESS. Capacitor C_{1f} only compensates inductances of the connecting cables and must be placed as close as possible to the elements *VT1, VT2, VT3* and *C*; its capacitance is considerably lower than that of C_f. Such a connection allows to exploit tram's radio-frequency filter L_{rf}, C_{rf} and input choke L_f for smoothing pulsed currents flowing from ESS to the overhead line.

The ESS is developed as an entirely autonomous device having no links to the tram control unit. Two current and two voltage sensors are used for ESS control purposes. Three of them

are placed inside of ESS and only tram input current sensor should be installed in the tram power circuit.
Fig. 2 shows the simplified four-axle tram T3A traction drive circuit with a DC chopper and DC traction motors in running, a) and braking, b) modes of operation.

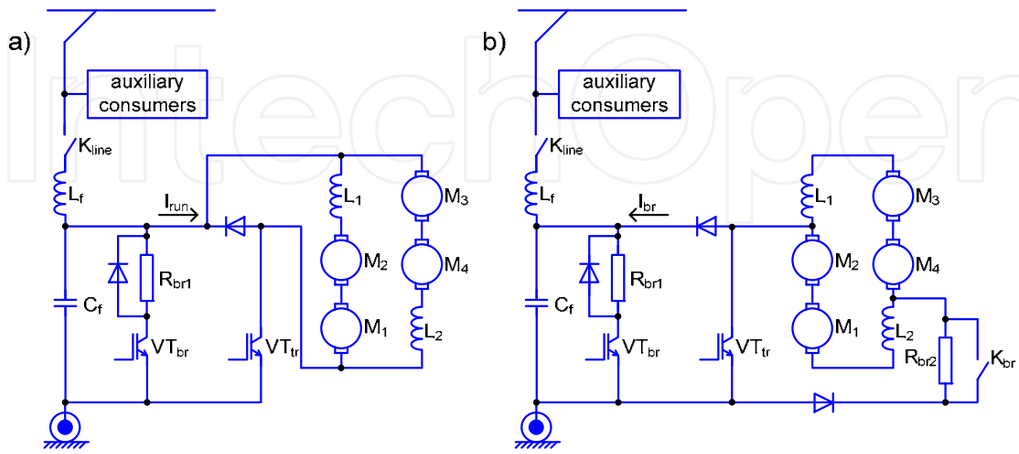

Fig. 2. A simplified circuit diagram of the tram T3A traction drive: a) in running mode, b) in braking mode.

IGBT VT_{tr} is a main switch for both buck (Fig. 2, a) and boost (Fig. 2, b) configurations of DC chopper. IGBT VT_{br} operates in a case when there are no consumers for the braking current I_{br}. Then voltage of capacitor C_f begins to rise and the tram control system works as the voltage stabilizer with a 780V setting. The energy is dissipated in the brake rheostat R_{br1}. This is the untapped energy which must be saved in ESS and then returned back when tram accelerates. When tram is braking at a high speed, the counter EMF of motors exceeds the supply voltage. To make the braking process controllable, an additional braking rheostat R_{br2} is included into the power circuit, which is short-circuited by contactor K_{br} when the speed falls below 30 km/h. The portion of braking energy dissipated in R_{br2} may be considered as a technological and for this type of drive cannot be saved in ESS.
The pulse currents of the DC chopper are closed through the capacitor C_f, whereas the overhead line current is smoothed by the choke L_f. Both transistors VT_{tr} and VT_{br} are steered by pulse width modulators with constant switching frequency 1000Hz.

3. Model of the tram traction drive with on-board ESS

The PSIM model of the T3A tram traction drive with installed on-board ESS is shown in Fig.3. The voltage source *V1* and diode *D1* represent the feeding substation and *R1* is an equivalent resistance of the connecting cables and overhead line. The current source *I2* simulates another tram connected to the same overhead line. The DC chopper of the tram is represented in two versions – as a continuous and a pulsed current source. In Fig. 3 the continuous current source *I1* is used. The positive direction of currents *I1* and *I2* shown in Fig. 3 corresponds to the running mode and negative – to the braking mode of operation of the both trams. The filter capacitor's voltage limiter (VT_{br} and R_{br1} in Fig. 2) is substituted with voltage source *V2*=780V and diode *D2*.

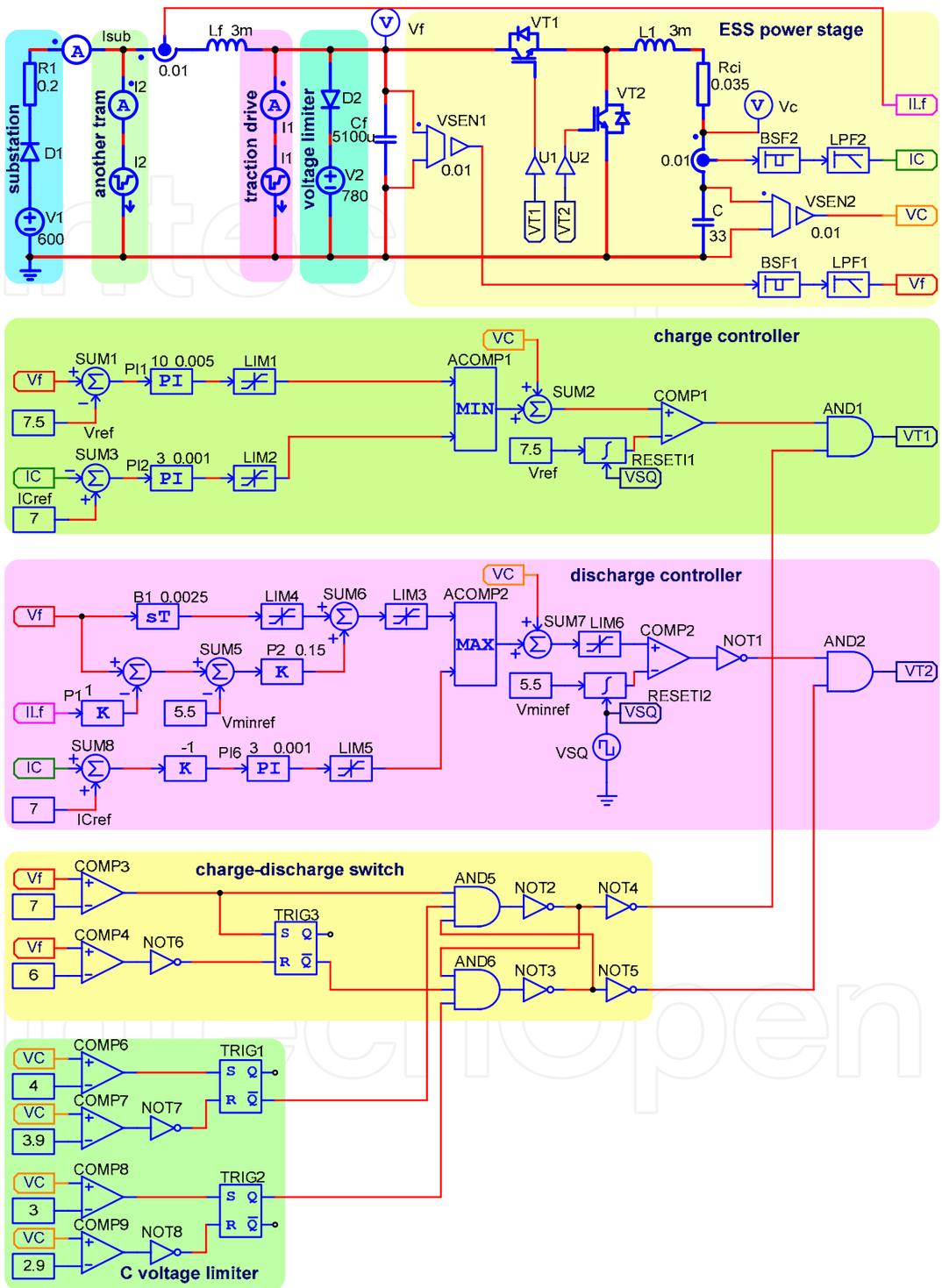

Fig. 3. PSIM model of an onboard ESS installed on the tram T3A

ESS power stage contains IGBTs *VT1* and *VT2*, choke *L1* and supercapacitor *C*. Since IGBT VT3 (see Fig. 1) is used only for protection purposes, it is eliminated from the PSIM model. The equivalent series resistance R_{Ci} of supercapacitor *C* is calculated for parallel connection of two modules containing 160 or 180 series-connected single capacitors *Maxwell* 3000F, 2.7V each, adding a 0.1mΩ connection resistance to the 0.29 mΩ internal resistance of a single capacitor.

Fig. 4 shows the pulsed current source model of the DC chopper while Fig. 5 explains principle of its operation. IGBTs VT_r and VT_b commutate current sources I_{DC1} and I_{DC2} to the output line forming positive or negative pulses of chopper current I_{ch} with a 500A amplitude. Pulse width is proportional to the steering voltage V_I which is compared with sawtooth voltage V_{saw} and its inverse value by comparators A1 and A2 respectively. V_{saw} has 1000Hz frequency and 5V amplitude.

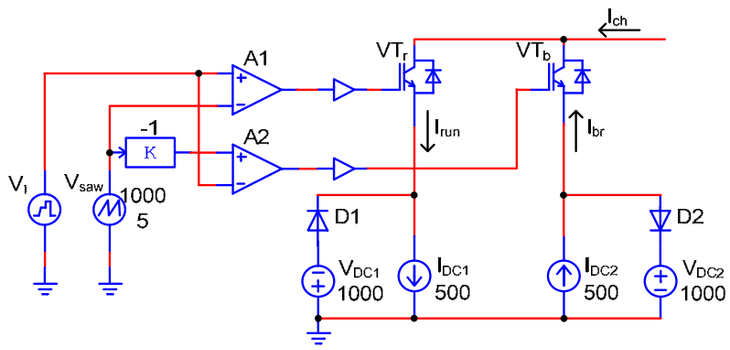

Fig. 4. PSIM model of the pulsed current source

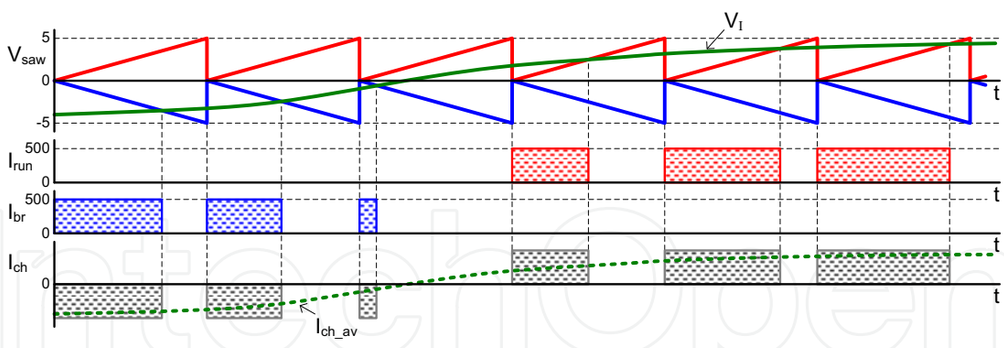

Fig. 5. Diagrams of the pulsed current source model

At positive values of the voltage V_I transistor VT_r operates and $I_{ch}=I_{run}$. At negative V_I operates VT_b and $I_{ch}=-I_{br}$. The average value of current pulses I_{ch_av} is proportional to V_I with scale 1V=100A. Voltage sources V_{DC1} and V_{DC2} and diodes *D1* and *D2* eliminate overvoltages when IGBTs are off.

The pulsed current source model noticeably increase simulation time that is why it is used only when interference between the tram DC chopper and ESS converter is investigated (see section 7).

4. ESS control system

Control system of ESS (see Fig. 3) contains supercapacitor charge controller, discharge controller, charge-discharge mode switch and supercapacitor voltage limiter.
The main task of the ESS controller is to store all tramcar braking energy not allowing its dissipation in a braking rheostat. To store the energy a capacitor must be discharged to the voltage V_{Cmin} at the beginning of braking. As the braking energy depends on the tramcar speed, the processes of charging and discharging the supercapacitor may be controlled in compliance with the tramcar's real speed. Unfortunately, such a control principle could not be provided in T3A tramcars due to the lack of a speed sensor.
Two voltages and two currents are measured for ESS control purposes: filter capacitor voltage V_f, supercapacitor voltage V_C, supercapacitor current I_C and tram input filter current I_{Lf}. Since filter capacitor voltage V_f and supercapacitor current I_C have 1000Hz ripple with significant amplitude, the measured signals are filtered by using 1000Hz band-stop filters *BSF1*, *BSF2* and low-pass filters *LPF1*, *LPF2* with cut-off frequency 800Hz.

4.1 Charge controller

A simplified equivalent circuit diagram of ESS in tram braking mode i.e. supercapacitor charge mode is shown on Fig. 6.

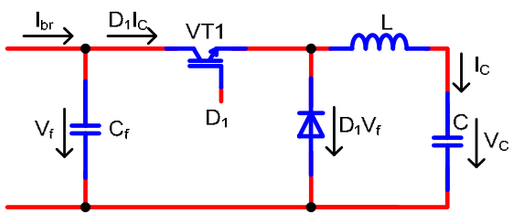

Fig. 6. A simplified circuit diagram of ESS in charge mode

For simplicity all circuit elements are suggested to be ideal and energy dissipative resistances are ignored. Voltages V_f, D_1V_f and currents I_C, D_1I_C are the average values with averaging interval being equal to the switching period of VT1, where D_1 is a duty ratio.
All braking energy will be saved in ESS if

$$D_1 I_C = I_{br} \tag{1}$$

Then capacitor C_f current is zero and voltage V_f is constant. Therefore, if the control system maintains the filter capacitor's voltage V_f constant, the controller automatically provides such a duty factor D_1 that Eq. (1) is valid. The setting for the filter capacitor's voltage V_{ref} must be selected slightly lower than 780 V. However, a second control loop is needed for the supercapacitor's current to limit it to an allowable level in the emergency cases when the braking power exceeds the rated value.
Assuming supercapacitor *C* as a voltage V_C source, the Fig. 4 circuit equations are

$$V_f(s) = \frac{1}{sC_f}(I_{br}(s) - D_1 I_C(s)) \; ; \tag{2}$$

$$I_C(s) = \frac{1}{sL}(D_1 V_f(s) - V_C) \tag{3}$$

Solving (2) and (3) for $V_f(s)$ and $I_C(s)$ yields

$$V_f(s) = \frac{sLI_{br}(s) + D_1 V_C}{s^2 LC_f + D_1{}^2} \tag{4}$$

$$I_C(s) = \frac{D_1 I_{br}(s) - sC_f V_C}{s^2 LC_f + D_1{}^2} \tag{5}$$

Equation (4) is an open-loop transfer function for the filter capacitor voltage V_f. Note that it depends nonlinearly on the control variable D_1. The open-loop system is stable and the steady-state voltage, obtained from (4) at s=0, $V_f\big|_{t=\infty} = V_C / D_1$, and steady state current obtained from (5) at s=0 $I_C\big|_{t=\infty} = I_{br} / D_1$. Hence, by choosing $D_1=D_{10}=V_C/V_{ref}$ feedforward may be introduced. It provides steady-state voltage $V_f=V_{ref}$ and facilitates performance of the feedback loop. The latter can be implemented by adding a small deviation d_1 to the duty ratio: $D_1=D_{10}+d_1$. The circuit diagram and operating principle of a pulse width modulator (PWM) with feedforward and feedback is shown in Fig. 7.

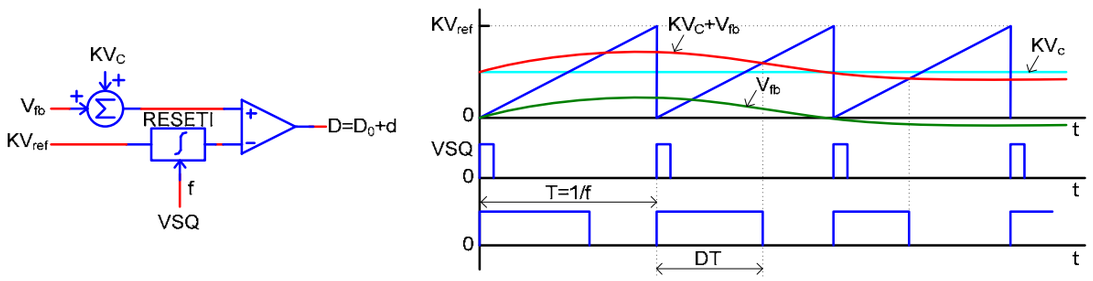

Fig. 7. A pulse width modulator with feedforward and feedback

Resetable integrator *RESETI* generates sawtooth voltage with switching period $T=1/f$ and amplitude KV_{ref}, where K is a gain of the voltage sensors. The pulse duty ratio at the comparator output $D=V_C/V_{ref}+V_{fb}/KV_{ref}=D_0+d$. Feedback voltage V_{fb} is bipolar and increase in V_{fb} causes increase in the duty ratio D and, as it results from (4), decrease in the filter capacitor voltage V_f. Such a PWM is used in both charge and discharge controllers.

The voltage control loop of the charge controller (see Fig. 3) consists of summator *SUM1*, proportional-integral (PI) controller *PI1* and voltage limiter *LIM1*. Reference voltage is set to V_{ref}=750V.

Supercapacitor current feedback is necessary for current limiting at allowable value which is set to I_{Cref}=700A. When current limiting takes place, all braking energy cannot be stored in ESS because $I_{br}>D_1 I_C$ and Eq. (1) is not valid. Voltage V_f raises up to value V_{fmax}=780V set by voltage limiter. Part of braking energy is dissipated in the braking rheostat (in voltage source V2 in Fig. 3). In this case transfer function for $I_C(s)$ is obtained from (3) substituting $V_f(s)=V_{fmax}$:

$$I_C(s) = \frac{1}{sL}(D_1 V_{f\max} - V_C) \tag{6}$$

The transfer function (6) is linear regarding to the control variable D_1 but an open-loop system is unstable.

Current control loop of the charge controller (see Fig. 3) consists of summator *SUM2*, PI controller *PI2* and voltage limiter *LIM2*. The feedback voltage applied to the pulse width modulator is the lesser of two control loop signals chosen by analogue comparator *ACOMP1*. In the voltage control mode $I_C < I_{Cref}$, the output signal of *LIM2* has the upper value and current control loop is disconnected. Similarly, in the current control mode $V_f > V_{ref}$, the output signal of *LIM1* has the upper value and the voltage control loop is disconnected.

4.2 Discharge controller

The equivalent circuit diagram of ESS in tram drive mode i.e. supercapacitor discharge mode is shown in Fig. 8. The I_{run} is an averaged current of the traction drive chopper in tram running mode.

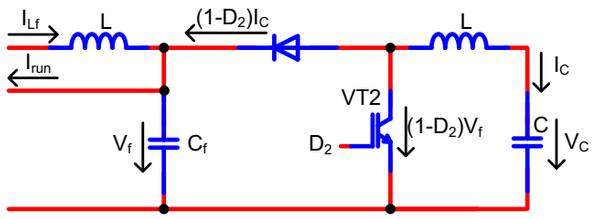

Fig. 8. A simplified circuit diagram of ESS in discharge mode

Suffering the same assumptions as in the previous section the circuit equations are

$$V_f(s) = \frac{1}{sC_f}((1-D_2)I_C(s) + I_{Lf}(s) - I_{run}(s)) \tag{7}$$

$$I_C(s) = \frac{1}{sL}(V_C - (1-D_2)V_f(s)) \tag{8}$$

Solving (7) and (8) for $V_f(s)$ yields

$$V_f(s) = \frac{(1-D_2)V_C + sLI_{Lf}(s) - sLI_{run}(s)}{s^2LC_f + (1-D_2)^2} \tag{9}$$

Equation (9) is very similar to (4) with $(1\text{-}D_2)$ instead of D_1. As $(1\text{-}D)$ is an inverted D, the same PWM may be used for discharge controller by adding logic inverter to the modulator output.

Supercapacitor current control loop is similar to that of the charge controller. The difference is in an opposite sign of the supercapacitor current and added analogue inverter.

Voltage control loop differs significantly from the charge controller because in the discharge mode ESS should have declivous VA characteristic. It is achieved with use of proportional (P) controller *P2* instead of PI controller and by adding input current I_{Lf} to the voltage feedback signal. Differentiator *B1* improves dynamic characteristics and stability of the

voltage feedback loop. Since duty ratio *(1-D)* decreases and voltage V_f increases with increase in the feedback voltage V_{fb}, the greater voltage of both control loops, chosen by analogue comparator *ACOMP2,* is applied to the PWM. Voltage reference for discharge mode is set V_{minref}=550V.

4.3 Charge-discharge switch

Charge-discharge mode switch is a very important part of the controller which vastly influences stable operation of ESS. The lack of running-braking mode signal due to autonomous conception of ESS complicates switch design, because information about tram drive mode should be extracted from the available measurements of currents and voltages. The objectives for choice of the proper charge-discharge switch solution are as follows:

- simultaneous setting of the both modes is not permissible,
- the circuit L_f, C_f, *L1* and *C* (Fig. 3) has a low damping factor and fast switching from one mode to other can cause rising oscillations in it,
- a neutral position – no mode is set, is permissible and is a good choice for achieving stable operation of the system,
- current I_{Lf} cannot help to determine tram drive mode and only filter voltage V_f should be used for it.

The charge-discharge switch is realized with two voltage comparators *COMP3*, *COMP4*, RS trigger *TRIG3* and a trigger build on the elements *AND5*, *AND6*, *NOT2…NOT5.* It's performance is illustrated in Fig. 9.

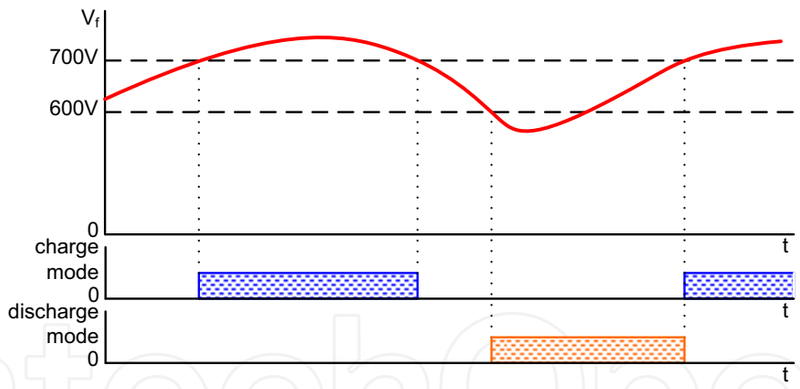

Fig. 9. Diagrams of charge-discharge mode signals

The charge mode is allowed when V_{Cf} >700V, but the discharge mode is set when voltage falls down to 600V level.

4.4 Supercapacitor voltage limiter

The maximum permissible voltage of supercapacitor V_{Cmax}=2.5*N*V has been chosen, where *N* is a number of series connected 2.7V 3000F capacitors. The minimum supercapacitor voltage V_{Cmin}=0.5V_{Cmax} has been commonly used e. g. (Barrero, R. et al, 2008 A) and is recommended by manufacturers of supercapacitors. Then 75% of its energy capacity is used at the power capability varying from $V_{Cmin}I_{Cref}$=0.5P_{max} to P_{max}. However, as it is discussed in (Latkovskis,

L. & Bražis, V., 2007), the braking power has its maximum at the beginning of tram braking when ESS has its minimum power capability. That is why more narrow voltage range has been chosen - $V_{Cmin} \approx 0.67 V_{Cmax}$. It yields 55% of the supercapacitor energy capacity to be utilized at power capability $0.67 P_{max}$ at the beginning of tram braking.
Supercapacitor voltage limiter consists of four voltage comparators *COMP6…COMP9*, two logic inverters *NOT7, NOT8* and two RS triggers *TRIG1, TRIG2*. Fig. 10 illustrates its operating principle.

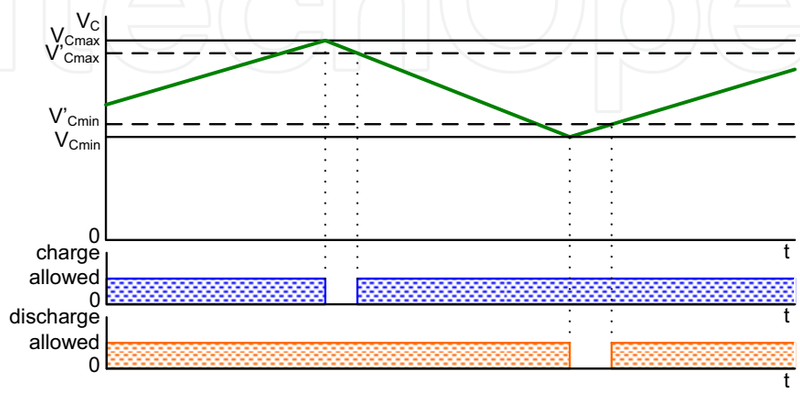

Fig. 10. Signal diagrams of supercapacitor voltage limiter

The charge mode is disabled when voltage reaches V_{Cmax}. It is permit again when voltage falls down to the level V'_{Cmax}. The discharge is disabled when supercapacitor voltage falls down to V_{Cmin}, and permit again when voltage rises up to V'_{Cmin}.
The resulting parameters of the supercapacitor bank and chosen voltage limiter settings for two parallel and *N* series connected single capacitors are shown in the Table 1.

N	C, F	R_{Ci}, mΩ	V_{Cmax}, V	V'_{Cmax}, V	V_{Cmin}, V	V'_{Cmin}, V	E, kJ
160	37.5	31.2	400	385	270	285	1633
180	33.3	35.1	450	430	300	320	1873

Table 1. Parameters of the supercapacitor bank and the voltage limiter settings

5. Optimization of the control system parameters

The first aim of the PSIM simulation was establishment of an optimal structure of the ESS control system and optimization of its feedback loop parameters to achieve stable operation and transient processes without overshoots and oscillations.
The filters *BSF1, BSF2, LPF1* and *LPF2* have been included in outputs of the voltage and current sensors, because presence of an AC component in the feedback signal causes nonlinearity of PWM and can be a reason of unstable operation of ESS. Second order band-stop filters *BSF1* and *BSF2* with 1000Hz central frequency eliminate the first harmonic of the ripple and low-pass filters *LPF1* and *LPF2* attenuate high order harmonics. Cut-off frequency 800Hz for *LPF1* and *LPF2* has been chosen as an optimal. At lower cut-off frequencies feedback performance worsens due to increased signal delay.

Parameters of PI controllers are optimized by frequentative simulation of ESS at different modes of operation using PSIM "parameter sweep" option. At chosen gain of the PI controller the time constant is varied. Then value of the time constant giving the best transient process is chosen and gain is varied. After some iteration the best combination of the gain and the time constant is found. The optimal values of control system parameters are shown in Fig. 3.

6. Simulation of ESS operation modes

The PSIM/Simulink simulation is performed for tramcar starting and braking processes in different situations with and without another tram connected to the overhead line. The typical load conditions in one overhead section are:

- single tram operation – only one tram is placed in overhead feeder section at low traffic density, no energy consumers and sources are available on DC line.
- two trams independent running – regenerative energy could be fully or partially used depending on both tram operation mode conditions,
- autonomous running in the case of net voltage unavailability.

If only one tram is running in overhead feeder section, then ESS supercapacitor capacity must be enough for storing the amount of one braking cycle energy. The braking energy could not be transferred to trams, which are supplied from other overhead sections and needs peak energy shaving. Such load situation is typical for Riga with city's radial tram lines system in suburban areas and single-track lines with exchange stops (lines 5 and 10), where no multiple tram driving at time is allowed in either direction.

The increase in number of simultaneously recuperating trams (more than 4-6) and presence of non-recuperating vehicles decreases the untapped regenerative energy (Latkovskis, L. & Grigans, L., 2008 B), therefore it is expected, that most difficult ESS working conditions would be if few trams are operated on two-track lines separated from other traffic outside city centre. Common situation on separated track is that the starting and braking is performed mostly at stops, when distance and consequently energy losses between two trams at the same stop are negligible, therefore the two tramcar energy exchange situation is chosen for simulation, where the braking and starting modes of both trams could been randomly shifted each from other. The model supposes, that tramcar with supercapacitor is working together in one feeder section with conventional T3A tram without any ESS. At low traffic density when single car trams are used, the conventional tram could start with its maximum traction current and brake with maximum braking current, which causes significant ESS voltage fluctuations. In the case, that double-car trams are used instead of single car, the power and current values doubles, but the shape of the characteristics remains the same if both coupled tramcars in each train-set have properly equal adjusted synchronised control systems.

The property of ESS to operate without overhead line voltage allows autonomous tram traction and braking. The autonomous traction is necessary for limited distances to restore interrupted traffic, e.g. in case of overhead damage, therefore the reduced performance of tram traction characteristics is allowed. The autonomous braking could eliminate regenerative energy losses, when tram passes overhead "dead" spots and switches.

For the simulation of ESS operation each tram is substituted with piecewise current source, which allows to change the number of tramcars by adding more sources without slowing

the modelling speed. The traction DC converter of the tram with ESS is substituted by continuous current source *I1* (see Fig. 3), conventional tram - with continuous current source *I2*. The current *I1* shape is taken from 51s long factory test measurements of maximum loaded tram with maximum acceleration and deceleration at speed 55km/h and braking current peak 480A. The tramcar traction DC buck converter provides acceleration from beginning of starting to 6s, and two stage field weakening from 6s to 39s, then follows regenerative braking from 39s to 51s, with additional resistance bypassing at 45s.

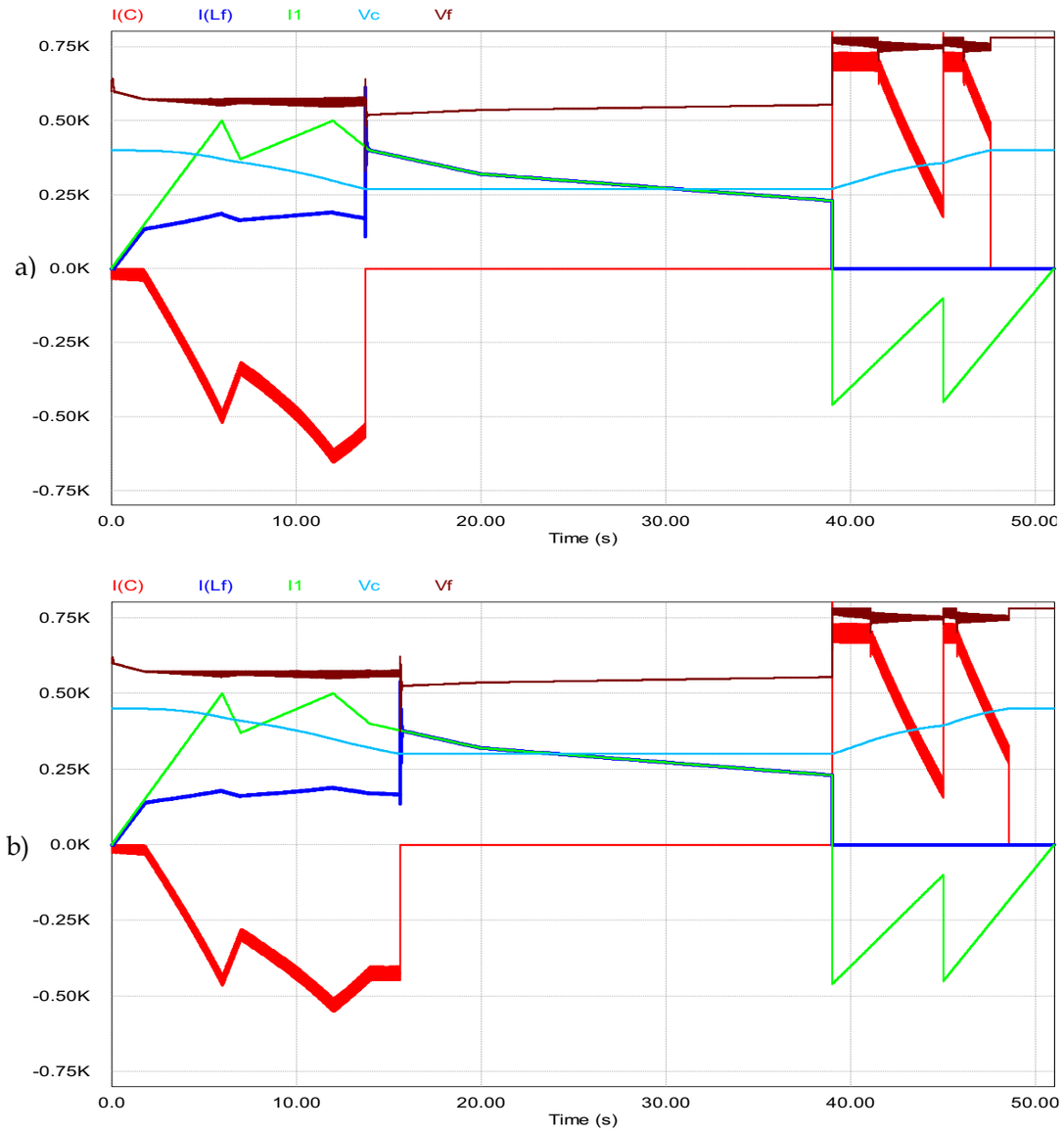

Fig. 11. PSIM simulation results of single tram for two values of supercapacitor capacitance: 37.5F (a) and 33.3F (b)

In the case of single tram operation current source *I2* value is set to zero. For research of two tram operation the current source *I2* diagram is shifted in time towards the first tram diagram, while the current shape is the same. In the autonomous mode of operation tram with ESS is disconnected from overhead line and other trams by setting the current source *I2* and the voltage source *V1* to zero.

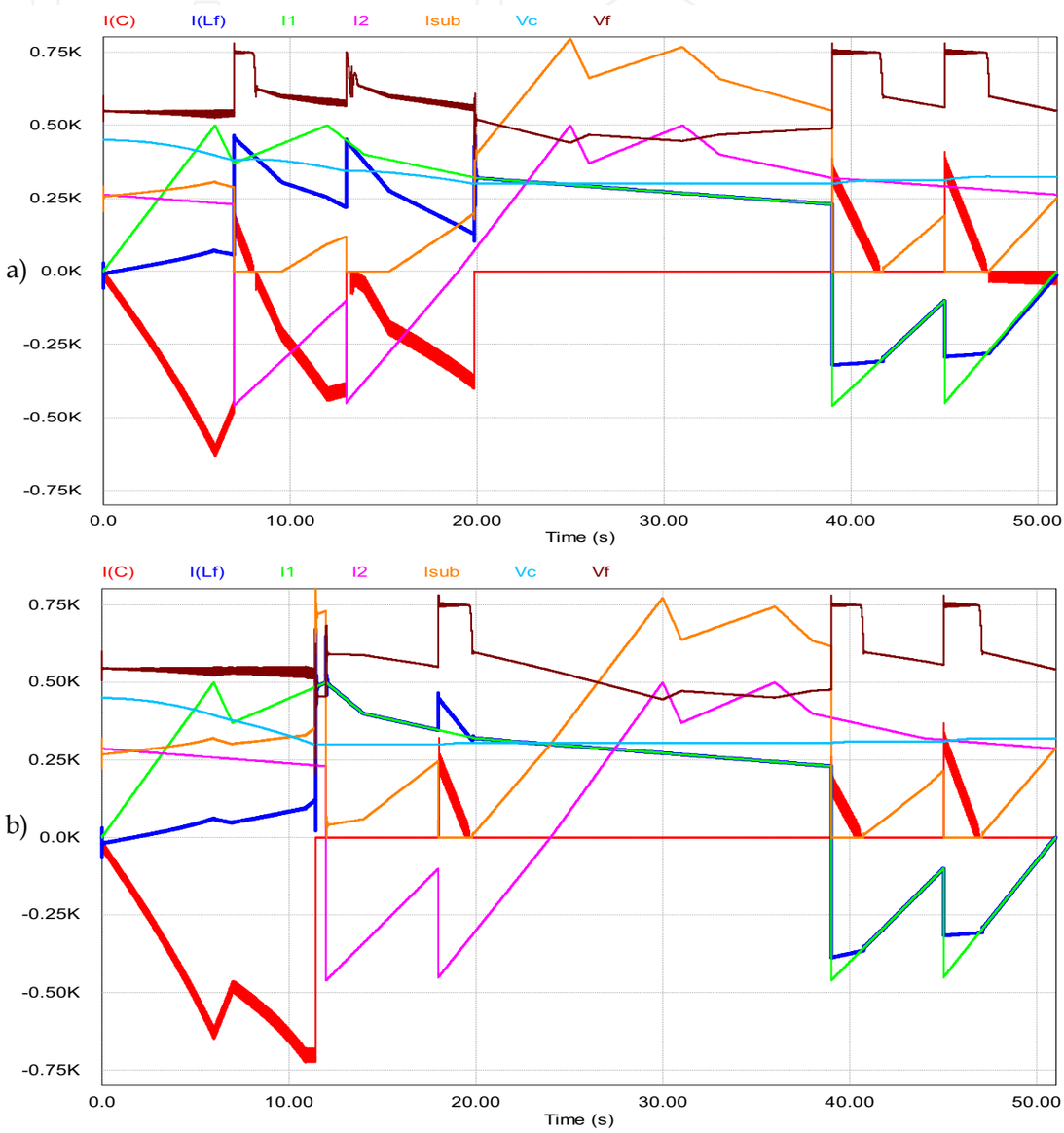

Fig. 12. PSIM simulation results of two tram operation at various tram starting time shift

The results of PSIM simulation for single tram with two variants of ESS supercapacitor capacitance 37.5F and 33.3F is shown in Fig. 11,a,b. Capacitance 33.3F has higher energy capacity and absorbs more energy due to the higher maximum and minimum voltage settings (see Table 1.), which allows to store more energy at the beginning of braking.

Therefore it ensures shorter time of current limiting, when regenerative energy partially is dissipated in braking rheostat. The power peak shaving time (the time of supercapacitor discharge to the minimum allowed voltage) with 33.3F supercapacitor is extended to 15.59s in comparison with 13.72s for 37.5F ESS capacitance. The total time of the current limiting at 700A level is 4s for 37.5F ESS and 3s for 33.3F ESS. The capacitance 33.3F is chosen for further simulations.

In the case of two trams independent running no current restriction is observed when one tramcar brakes (Fig. 12.). The excessive regenerative energy is transferred to ESS from both trams. The shift between starting moments of the both trams strongly influences the regenerative energy transferring. If the second tram begins braking at the moment of the first tram field weakening (Fig. 12., a.), this causes the ESS charging with surplus energy in time interval 7s...8s. Due to peak shaving the substation maximal current is significantly reduced to 306A and even in time intervals 7s...9.6s and 12s...15.4s $I_{sub}=0$. The ESS converter switching between charging and discharging modes passes without unstable oscillations. Fig. 12, b shows the case when another tram brakes at second stage of field weakening of the first tram. It causes shorter supercapacitor discharge time (12s) because both trams operate in the traction mode for longer time.
Simulation results of tram autonomous operation are shown in Fig. 13. Due to the restricted ESS capacity the autonomous traction with maximum traction current is possible up to first 9s, when supercapacitor voltage drops close to the lower limit and filter capacitor voltage decreases to 500V. It corresponds to vehicle speed approximately 27km/h.

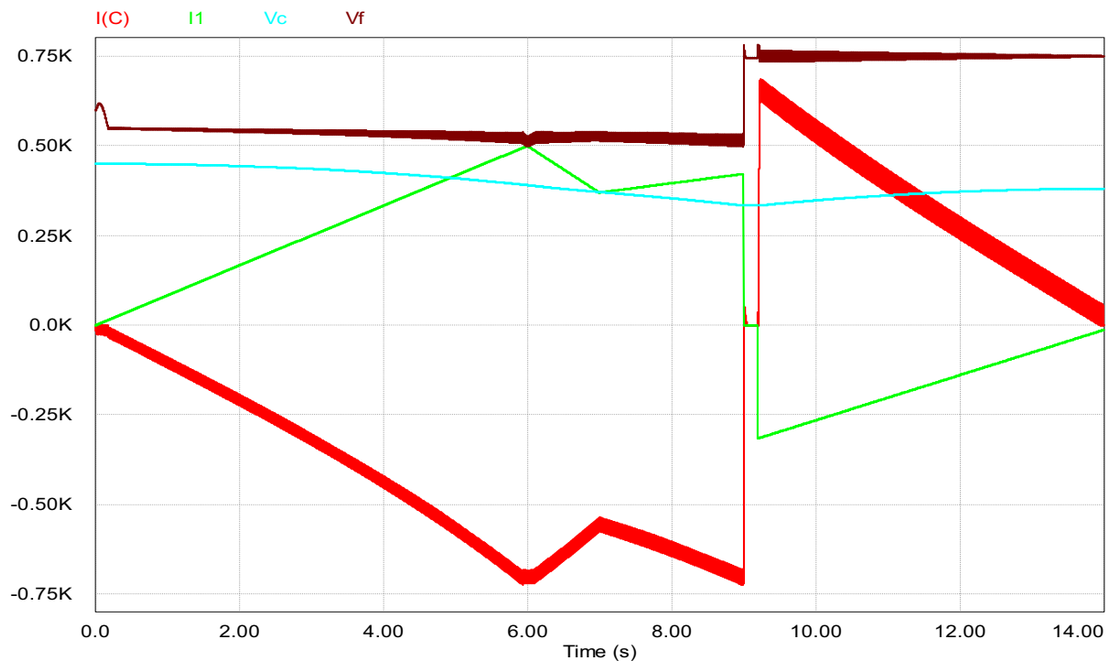

Fig. 13. PSIM simulation of tram autonomous operation

Because the prolonged traction with field weakening due to limited ESS power is impossible, it's recommended to restrict the autonomous traction with DC motor full field connection only (up to 6s acceleration time with speed 20-25km/h). The 0.2s long switching from traction to braking mode is stable and not significantly different from simplified instant mode switching.
Overhead voltage failure at different stages of tram movement also has been simulated. Fig. 14 shows a case when overhead voltage failure happened at 42s, when tram was braking at full speed. One can ensure that it didn't cause abnormal operation of tram equipment.

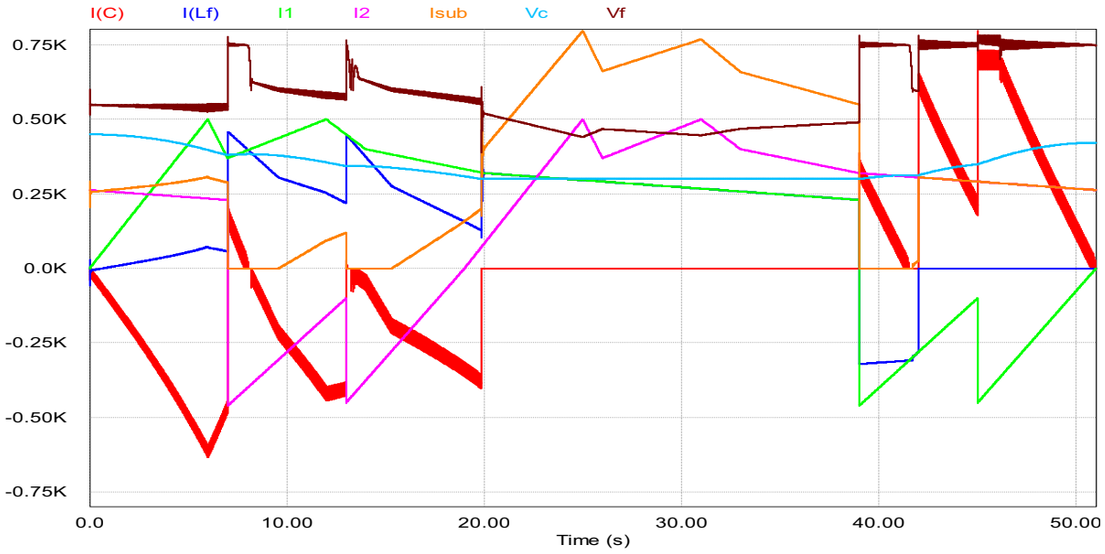

Fig. 14. Simulation of overhead voltage failure at tram braking (42s)

The ESS cannot store all regenerative braking energy if tramcar maximum traction and braking currents are taken from the factory tram test methodology, but in real traffic conditions the maximum acceleration and deceleration values are not widely observed. Fig. 15 shows the 300s long drive test simulation with currents *I1* and *I2* recorded on tram T3A running in line Nr 6. ESS accumulates all braking energy even when two trams are braking simultaneously (275-285s).

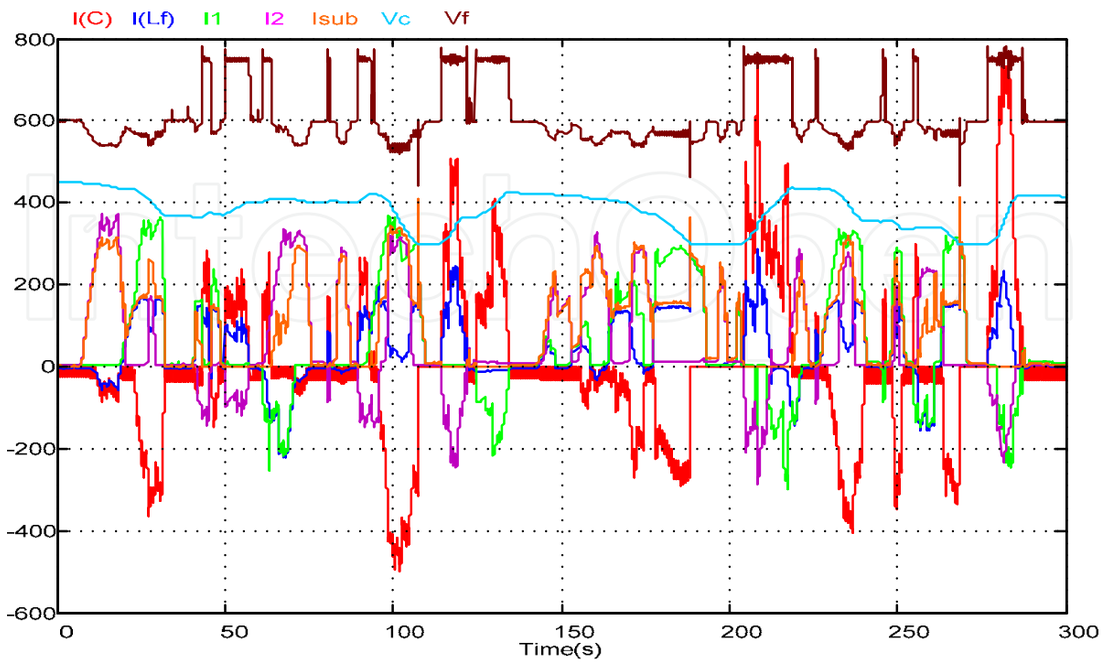

Fig. 15. PSIM/Matlab simulation of tram operation in real traffic driving conditions

7. Interaction between ESS and traction converter

By applying a pulsed current PSIM model of DC PWM tram converter the control system's stability is investigated in both synchronous and asynchronous operation modes of the tram DC converter and ESS current controller. In the section 6 for faster and simplest simulation the tram power scheme was substituted by linear current supply. In the real situation tram DC converter generates current pulses with 1000Hz frequency with almost constant amplitude and variable pulse width. Filter capacitor C_f is common for both converters. Due to its relatively small capacitance (5100μF) current pulses causes considerable capacitor voltage ripple which can affect performance of the energy storage device. The aim of PSIM simulation is:

- to investigate how the interference between two converters affects performance of the voltage control loop,
- to optimize parameters of PID control loops,
- to ascertain whether the action of both converters should be synchronized or not.

In synchronous operation mode the tram DC converter and ESS switching frequency is set 1000Hz. The asynchronous operation is tested in two modes with small and great difference in converter frequencies, where the tram DC converter frequency is set correspondingly 1001Hz and 1005Hz. The ESS converter frequency always remains 1000 Hz.

Because the autonomous traction could be provided with limited speed, the correct comparison of converter operation modes at various tram load conditions could be made only with acceleration at full DC motor field up to 25km/h (6s starting time) and braking from this speed. Such restriction also helps to reduce simulation time.

Fig. 16 demonstrates the interaction between ESS and single tramcar traction converter in synchronous mode of operation.

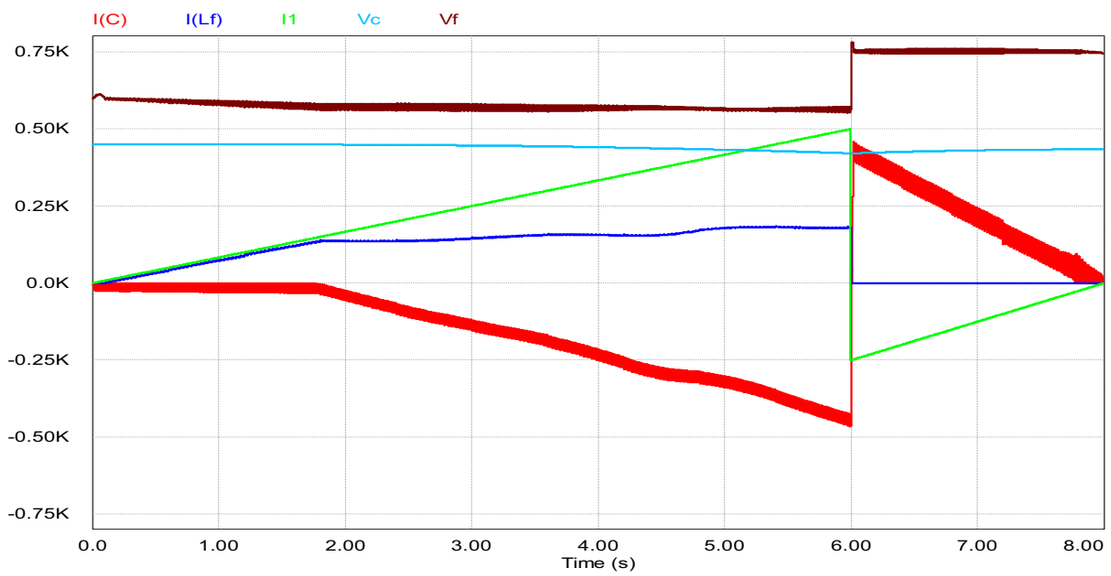

Fig. 16. Interaction between ESS and traction converter in synchronous operation mode

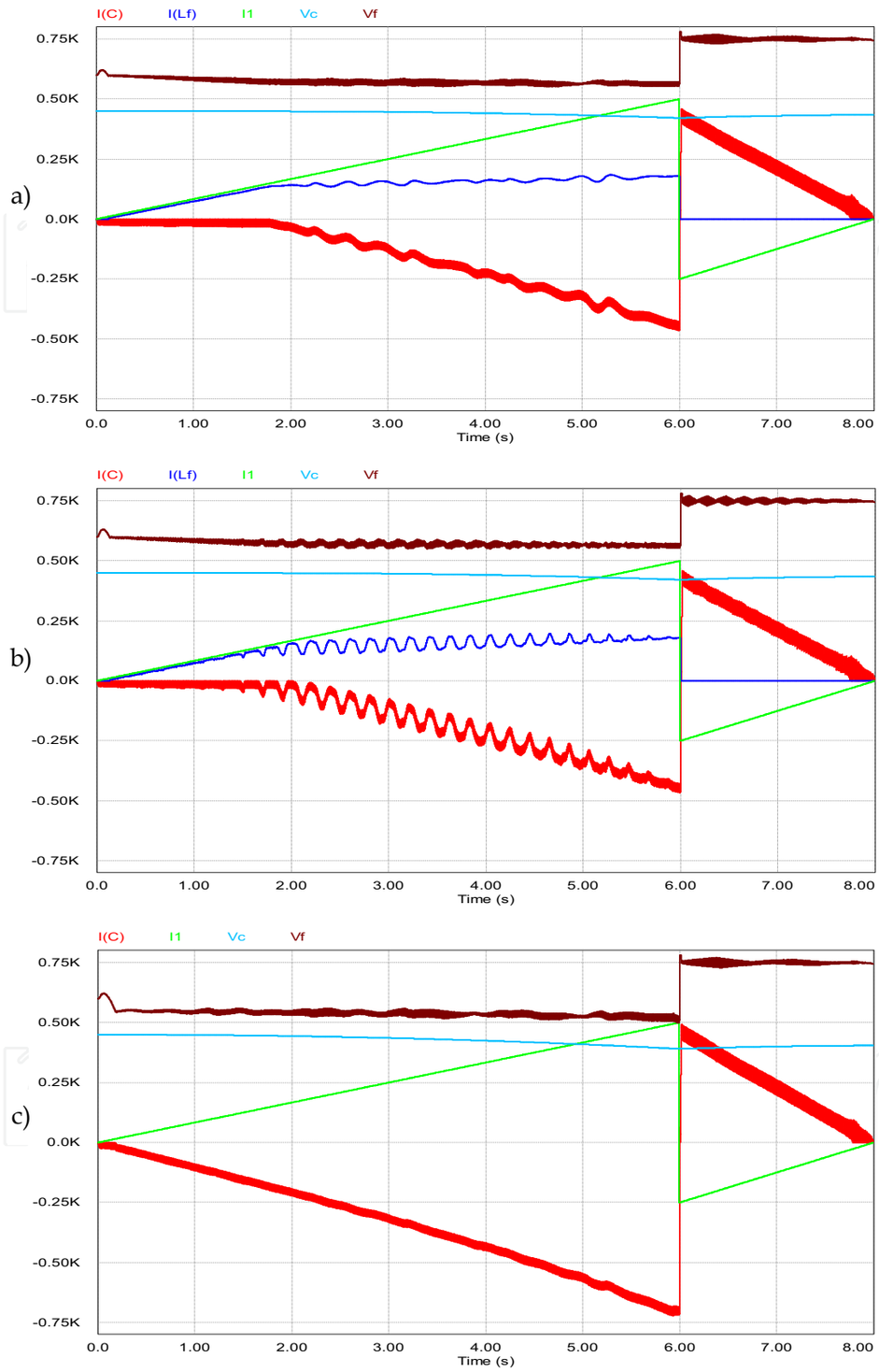

Fig. 17. Asynchronous operation mode with 1Hz (a) and 5Hz (b) difference in both converter switching frequencies, and autonomous traction mode (c) with 1Hz difference

The same situation in asynchronous operation mode with 1Hz (a) and 5Hz (b) difference in switching frequencies of the both converters is shown in Fig. 17. Fig. 17,c demonstrates autonomous traction with 1Hz difference in converter switching frequencies. The width of curves for the voltage V_f and current I_C in Fig. 17 is equal to their ripple amplitudes.
Analysing obtained results of pulsed current source simulation and comparing them to that of simulation with continuous DC current source the following conclusions has been made:

- no significant difference in currents and voltages between the case with continuous DC current and pulse current source is observed,
- the final charge of the supercapacitor is the same in all cases; efficiency factor of the energy storing ≈0.96 has been achieved,
- observed voltage V_f ripple amplitude oscillations is a result of interference between two pulsed current sources with different frequencies 1001Hz and 1000Hz and is not caused by control systems instability,
- although the voltage ripple in the voltage PID control loop is significant, it does not cause malfunction of the control system in the both synchronous and asynchronous operation modes of the traction and the energy storage converters.

One can observe that the mode of operation (synchronous or asynchronous) does not affect considerably process of the supercapacitor charging if difference in frequencies does not exceed 1Hz. At 5Hz difference supercapacitor and line current ripples become significant.
Fig. 18 shows waveforms of the chopper current $I1_{pulse}$, switch current $I_{(VT1)}$, supercapacitor discharging current I_C and filter capacitor voltage V_f in an asynchronous mode of operation with 1Hz difference in the switching frequencies of the both converters and expanded scale of time.

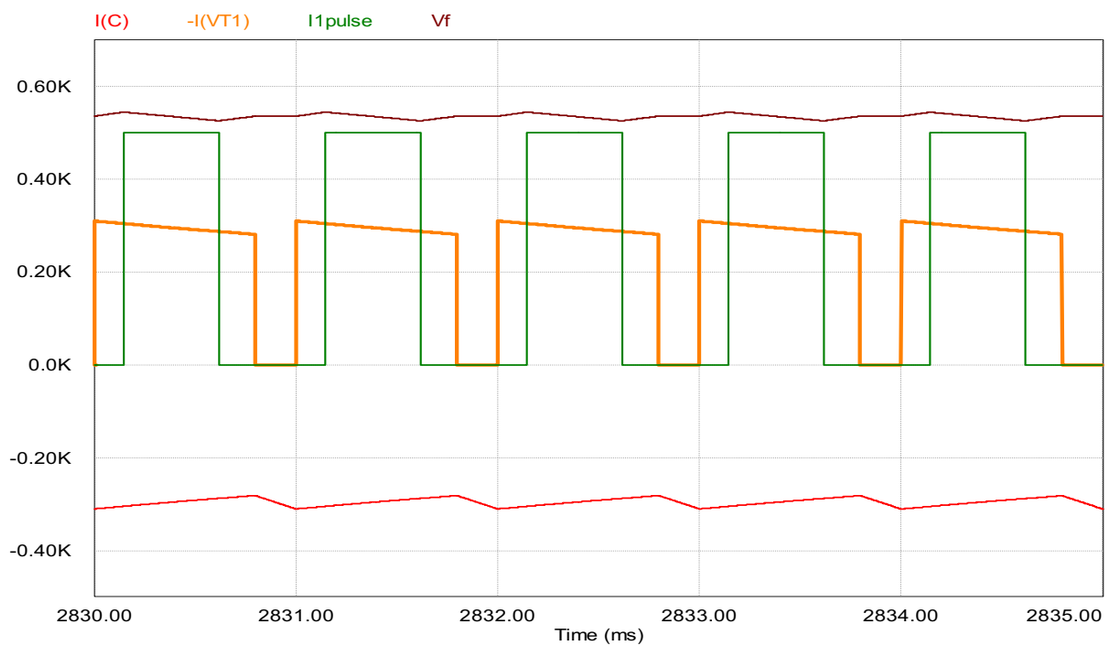

Fig. 18. Voltage and current diagrams in an asynchronous operation mode of ESS and traction converter

One can ensure that the voltage V_f and current I_C ripples are caused by the switched-mode operation of the power converters and are not a result of instable operation of the energy storage device control system. The precision of tram control system quartz clock signal ensures less than 1Hz difference between both converter working frequencies; however low frequency oscillations with frequency up to 5Hz could occur due to the control system adjusting restrictions.

8. Conclusion

1. Simulation results show stability of ESS control system in all operation modes, and ESS ability to utilize braking energy of the tram with high efficiency.
2. Installation of a supercapacitor in a T3A tramcar allows storing efficiently all the energy returned during the braking time independently of other overhead-connected consumers.
3. The complete braking energy storage is provided if in the ESS controller the filter capacitor voltage feedback is introduced. To limit the supercapacitor current to an allowable level a current control loop is needed as well.
4. The difference between synchronous and asynchronous mode of converters operation is insignificant if difference in switching frequencies of the tram DC chopper and ESS converter does not exceed 1Hz. Such accuracy can be easy achieved by using quartz oscillators; therefore the synchronization of both converter switching frequencies is not necessary.
5. Although ESS and tram traction converter control systems are independent, this causes drawbacks – complicated operation algorithms of the ESS control system that reduce its stability margin.
6. For better recognition of tram driving modes and oscillation dampening the control system must be upgraded with speed sensor. When ESS is developed for brand-new tramcar, the ESS and traction converter control systems must be synchronised. Tram control system commands must be sent to ESS controller.
7. The future research could be done for the ESS and tram control system integration in automatic traffic control and signalisation system, which allows to collect and predict information about braking energy amount and even manage optimal multiple tram traffic.

9. References

Barrero, R.; Tackoen, X.; Van Mierlo, J. (2008 A). Analysis and configuration of super-capacitor based energy storage system on-board light rail vehicles. *Proceedings of the 13th International Power Electronics and Motion Control Conference EPE-PEMC 2008*, Poznan, 1-3 September 2008, pp. 1535-1540.

Barrero, R.; Tackoen, X.; Van Mierlo, J. (2008 B). Improving energy efficiency in public transport: Stationary supercapacitor based Energy Storage Systems for a metro network *Vehicle Power and Propulsion Conference, VPPC '08.* IEEEDate: 3-5 Sept. 2008, Pages: 1 – 8

Destraz, B.; Barrade, P.; Rufer, A.; Klohr, M. (2007) Study and simulation of the energy balance of an urban transportation network. *European Conference on Power Electronics and Applications*, *EPE 2007*, 2-5 Sept. 2007, Pages: 1 - 10 Digital Object Identifier 10.1109/EPE.2007.4417349

Joller, J. (1998). Research of trams traction drives. Baltic Electrical Engineering Review 1 7, Vilnius, pp. 17–20.

Latkovskis, L.; Bražis, V. (2007). Application of supercapacitors for storage of regenerative energy in T3A tramcars. *Latvian Journal of Physics and Technical Sciences*, *Riga*, N5, pp. 23-33, ISSN 0868-8257.

Latkovskis, L.; Bražis, V. (2008). Simulation of the Regenerative Energy Storage with Supercapacitors in Tatra T3A Type Trams. *Proceedings of the Tenth International Conference on Computer Modeling and Simulation (UKSIM 2008),* Cambridge, UK, 1-3 April 2008, pp. 398-403.

Latkovskis, L.; Grigans, L. (2008 A). A Method for Estimation of the Untapped Regenerative Braking Energy in Urban Electric Transport. *CD-ROM of Conference of Young Scientists on Energy Issues CYSENI 2008*, Kaunas, May 2008, pp. IV-41 – IV-48.

Latkovskis, L.; Grigans, L. (2008 B). Estimation of the Untapped Regenerative Braking Energy in Urban Electric Transportation Network. *Proceedings of the 13th International Power Electronics and Motion Control Conference EPE-PEMC 2008*, Poznan, 1-3 September 2008, pp. 2089-2093.

Rankis, I.; Brazis, V. (2000). Simulation of tramcar's energy balance. *2nd Intern. Conf. "Simulation, Gaming, Training and Business Process Reengineering in Operations",* Riga, pp. 160–163.

Rufer, A. (2003). Power-Electronic Interface for a Supercapacitor-Based Energy-Storage Substation in DC-Transportation Networks. *EPE Conference proceedings* Toulouse, pp. D1–D8.

Szenasy, I. (2008). Improvement the energy storage with ultracapacitor in metro railcar by modeling and simulation. *Vehicle Power and Propulsion Conference*, *VPPC '08*. IEEEDate: 3-5 Sept. 2008, Pages: 1 – 5.

Sejin, N.; Jaeho, Ch.; Hyung-Cheol, K.; Eun-Kyu, L. (2008). PSiM based electric modeling of supercapacitors for line voltage regulation of electric train system. *Power and Energy Conference, PECon 2008.* IEEE 2nd International Date: 1-3 Dec. 2008, Pages: 855 – 859.

IntechOpen

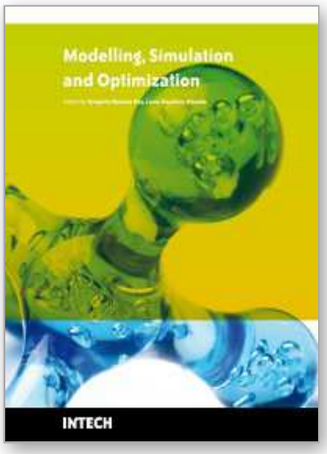

Modelling Simulation and Optimization

Edited by Gregorio Romero Rey and Luisa Martinez Muneta

ISBN 978-953-307-048-3
Hard cover, 708 pages
Publisher InTech
Published online 01, February, 2010
Published in print edition February, 2010

Computer-Aided Design and system analysis aim to find mathematical models that allow emulating the behaviour of components and facilities. The high competitiveness in industry, the little time available for product development and the high cost in terms of time and money of producing the initial prototypes means that the computer-aided design and analysis of products are taking on major importance. On the other hand, in most areas of engineering the components of a system are interconnected and belong to different domains of physics (mechanics, electrics, hydraulics, thermal...). When developing a complete multidisciplinary system, it needs to integrate a design procedure to ensure that it will be successfully achieved. Engineering systems require an analysis of their dynamic behaviour (evolution over time or path of their different variables). The purpose of modelling and simulating dynamic systems is to generate a set of algebraic and differential equations or a mathematical model. In order to perform rapid product optimisation iterations, the models must be formulated and evaluated in the most efficient way. Automated environments contribute to this. One of the pioneers of simulation technology in medicine defines simulation as a technique, not a technology, that replaces real experiences with guided experiences reproducing important aspects of the real world in a fully interactive fashion [iii]. In the following chapters the reader will be introduced to the world of simulation in topics of current interest such as medicine, military purposes and their use in industry for diverse applications that range from the use of networks to combining thermal, chemical or electrical aspects, among others. We hope that after reading the different sections of this book we will have succeeded in bringing across what the scientific community is doing in the field of simulation and that it will be to your interest and liking. Lastly, we would like to thank all the authors for their excellent contributions in the different areas of simulation.

Slavka Krautzeka 83/A
51000 Rijeka, Croatia
Phone: +385 (51) 770 447
Fax: +385 (51) 686 166
www.intechopen.com

No.65, Yan An Road (West), Shanghai, 200040, China
中国上海市延安西路65号上海国际贵都大饭店办公楼405单元
Phone: +86-21-62489820
Fax: +86-21-62489821

IntechOpen

IntechOpen